Received: 12 August 2024 | Revised: 11 September 2024 | Accepted: 11 September 2024

DOI: 10.1002/jsde.12800

ORIGINAL ARTICLE

AOCS WILEY

Properties of liquid foams stabilized by sugar-based surfactants and prepared under different conditions

João Victor Cordeiro do Nascimento[1] | Eduardo R. A. Lima[1] | Natalie Preisig[2] | Cosima Stubenrauch[2]

[1]Physical Chemistry Department, Institute of Chemistry, Rio de Janeiro State University—UERJ, Rio de Janeiro, Brazil

[2]Institute of Physical Chemistry, University of Stuttgart, Stuttgart, Germany

Correspondence
Cosima Stubenrauch, Institute of Physical Chemistry, University of Stuttgart, Stuttgart, Germany.
Email: cosima.stubenrauch@ipc.uni-stuttgart.de

Funding information
Coordenação de Aperfeiçoamento de Pessoal de Nível Superior, Grant/Award Number: 001

Abstract

The study of foam stability is a subject of continuous research, due to the different fields of application foams are used in. In this study, foams stabilized with a family of nonionic sugar-based surfactants were investigated systematically. For this purpose, we changed the concentration (c > cmc), the gas flow rate, and the disk porosity. The foam properties were evaluated by measuring the foam volume, the liquid fraction, and the bubble size distribution as a function of time. We observed good foamability for all conditions tested with a tendency towards increasing stability with increasing chain length and increasing head group size. For foams stabilized by the short chain surfactants β-C_8G_1 and β-C_8G_2 we observed a significant time evolution due to coarsening and coalescence, while foams stabilized with the longer chain surfactants hardly changed during the observation time. From an industrial point of view, our study helps to understand properties of foams generated under different conditions. We conclude that for the special family investigated here a very good performance can be expected for a broad variety of conditions.

KEYWORDS
application of surfactants, foaming properties, sugar-based surfactants

INTRODUCTION

Once one disperses gas into a liquid, a liquid foam might be generated (Encyclopedia of Chemical Technology. *12*, 2005; Rossen, 1996; Saint-Jalmes, 2006; Weaire & Hutzler, 1999). Liquid foams are present in many applications, such as detergency, food, cosmetics, firefighting, oil recovery, or flotation of minerals. Liquid foams are also used as template for the synthesis of solid foams (Andrieux et al., 2018; Stubenrauch et al., 2018).

Among a large variety of surfactants applied worldwide, those that originate from renewable resources have been intensively studied due to sustainability and an environment-friendly demand (Bhadani et al., 2020; Bois et al., 2020). This includes sugar-based surfactants (Stubenrauch, 2001). Sugar-based surfactants consist of a hydrophobic alkyl chain and a hydrophilic glucose ring. They are found in starch, sugar beet or sugarcane, and have been extensively investigated in many applications, such as pharmaceutical formulation, cosmetic, food and personal care products because of their mild character, biodegradability and functional properties (Bois et al., 2020; Carnero Ruiz, 2008; Hill & Rhode, 1999; Tesmann et al., 1996; Von Rybinski & Hill, 1998). Using sugar-based surfactants one may end up in colloidal systems with good wetting, foaming, and emulsifying performances (Bhadani et al., 2020; Carnero Ruiz, 2008; Gaudin, Rotureau, et al., 2018; Lourith & Kanlayavattanakul, 2009; Rojas et al., 2009; Yoshimura et al., 2013).

Two types of measurements are often used in foaming studies: foamability, which is the foam generation power of a solution, and foam stability, which stands for the lifetime of a foam after its generation (Stubenrauch et al., 2009). While the former is related to the nature of the surfactant and its concentration in the solution (Engels et al., 1998; Prins, 1992; Pugh, 1996; Rosen, 2004; Shinoda et al., 1961; Stubenrauch et al., 2009), the latter is limited by drainage of the liquid

inside the foam, Ostwald ripening, and coalescence (Ekserova & Kruglíàkov, 1998; Pugh, 1996; Sadoc et al., 1999).

Being able to control the factors that affect foam stability, one can deliberately increase or decrease foam stability. Examples are (i) an increase of the liquid's viscosity or the surface viscoelasticity to slow down drainage (Pugh, 1996; Stubenrauch et al., 2009); (ii) a reduction of the gas bubbles polydispersity, of the water solubility of the gas, and of the gas permeability through the surfactant layer to slow down Ostwald ripening (Prud'homme & Khan, 1996); and (iii) boost the resistance to rupture of the foam films through high disjoining pressure and high surface viscoelasticity (Kim et al., 1997; Santini et al., 2007; Stubenrauch & Miller, 2004; Tadros, 2007; Tamura et al., 1995; Ting et al., 1984).

As regards sugar-based surfactants, lots of research was done in order to better understand structure—property relationships in general and the relationship between molecular structure and surface and self-assembling properties in particular (Bois et al., 2023; Gaudin, Lu, et al., 2019). Moreover, studies to develop predictive models were carried out to correlate surface properties with the molecular structure of sugar-based surfactants (Gaudin et al., 2016; Gaudin, Fayet, et al., 2018; Gaudin, Lu, et al., 2019; Gaudin, Rotureau, et al., 2018; Gaudin, Rotureau, et al., 2019). However, relatively few studies about foam properties and foam film properties were conducted. For instance, Stubenrauch (Boos, Preisig, et al, 2013; Grigoriev & Stubenrauch, 2007; Stubenrauch et al., 2007, 2010), Muruganathan et al. (2004) and Zhao et al. (2018) have extensively investigated the foaming properties of *n*-dodecyl-*β*-maltoside, which included microscopic arrangement of the surfactant at the air/water interface, rigidness, thickness, stability and viscoelasticity of the foam film. In addition, the influence of the surfactant's molecular structure on the foaming properties of alkylpolyglycosides (Bois et al., 2023; Ware et al., 2007) was investigated. Bois et al. (2023) carried out promising research about the foaming behavior of 17 sugar-based surfactants. They analyzed the foamability, the foam stability and the maximum foam density of foams which were generated with the gas sparging method. By gradually changing the surfactant structure it was possible to correlate the foaming behavior of glycolipids to the surfactant concentration and the interfacial properties, by using *Principal Component Analysis* (Method of projection of independent variables, inter-correlated at some order, into a set of non-inter-correlated variables for development of predictive linear and non-linear regressions between the parameters involved).

The above-mentioned study from Bois, however, was conducted at bulk concentrations from $c = 0.001$cmc to $c =$ cmc for each surfactant. At these low concentrations depletion effects (Boos et al., 2012) must be considered which the authors overlooked: it is only at concentrations well above the cmc that new surface areas can be generated without changing the bulk concentration. Following this line of thinking, the foam measurements presented in the study at hand were carried out well above the cmc. We studied the foaming properties of 5 sugar-based surfactants, with different alkyl chain lengths and glucose units. We used the gas sparging method and investigated foamability and foam stability. In the latter case we measured the time evolution of the liquid fraction, the foam volume, and of the bubble size distribution. Furthermore, different experimental conditions were tested, namely different surfactant concentrations, different disc porosities, and different gas flow rates, for evaluating how they affect the foaming properties of the surfactant solutions.

MATERIALS AND METHODS

Chemicals

From Glycon a family of 7 nonionic sugar-based surfactants was purchased: *n*-octyl-*β*-glucoside (β-C_8G_1), *n*-octyl-*β*-maltoside (β-C_8G_2), *n*-decyl-*β*-glucoside (β-$C_{10}G_1$), *n*-decyl-*β*-maltoside (β-$C_{10}G_2$), *n*-dodecyl-*β*-glucoside (β-$C_{12}G_1$), *n*-dodecyl-*β*-maltoside (β-$C_{12}G_2$) and *n*-tetradecyl-*β*-maltoside (β-$C_{14}G_2$). Each of them was used as received. NaCl (purity above 99%) was obtained from Merck. The glassware used was cleaned with deconex 22 LIQ-x from Borer Chemie AG and rinsed several times with doubly distilled water. All the solutions were made with doubly distilled water at room temperature (22°C). In Table S1 we listed the molecular structures, molar masses, and cmc-values at room temperature of the nonionic sugar-based surfactants studied.

Foam measurements

The FoamScan (TECLIS, France) was used to carry out the foam measurements. Image analysis and conductivity measurements were used to determine the foamability, the foam stability, the liquid fraction, and the bubble size distribution.

In each experiment 120 mL of foam was formed in a glass column by sparging nitrogen (N_2) at a constant flow rate through a porous disk placed on the bottom of the column. For each run 60 mL surfactant solution were filled into the column. We carried out foam measurements with (1) different surfactant concentrations (2 cmc, 5 cmc, and 10 cmc), (2) different gas flow rates Q (20, 40, 60, and 84 mL min^{-1}) and (3) different disk porosities (P1 with pore sizes of Ø = 101–160 μm, P2 with Ø = 41–100 μm, P3 with Ø = 17–40 μm). For each surfactant 250 mL solution was prepared for a triplicate experiment. The duration of each run was up to 3600 s.

The foam volume was monitored by a CCD (Charged-Couple Device) camera, while the conductivity of the solution Λ_{bulk} and the foam Λ_{foam} were measured by using electrodes at fixed positions of the

column. To ensure conductivity we added 10^{-2} M of NaCl to each surfactant solution. The liquid fraction ε of the foam was determined by using empirical Equation (1) provided by Feitosa et al. (2005).

$$\varepsilon = 3\sigma_{el}\left(\frac{1+11\sigma_{el}}{1+25\sigma_{el}+10\sigma_{el}^2}\right), \quad (1)$$

with σ_{el} being relative electrical conductivity.

$$\sigma_{el} = \frac{\Lambda_{\text{foam}}}{\Lambda_{\text{bulk}}}. \quad (2)$$

With an additional CCD camera at the wall of the glass column and the cell size analysis (CSA) software one can visualize and evaluate the change of the bubble size and of the bubble size distribution over time. The CSA software calculates the bubble radius r from the cross-sectional area of the bubbles on the column wall, assuming that all bubbles are spherical. The number of bubbles in an observed area, the arithmetic mean bubble radius $<r>$, and the polydispersity index (PI) were calculated at different times:

$$PI = \frac{\sqrt{(<r^2> - <r>^2)}}{<r>}. \quad (3)$$

Before using the CSA software, bubble images were treated with the freeware program ImageJ to obtain a water-free skeleton by reducing the dark lines on the surface plateau borders to a line of one-pixel width (for more detail see Boos et al., 2012; Boos, Drenckhan, et al., 2013). Pictures of foam bubbles taken directly after stopping the gas spreading ($t = 0$ s) are shown in Figure 1. Additional information concerning the experimental procedure are given in the SI.

RESULTS AND DISCUSSION

The main focus of this study was to measure how foamability and foam stability are affected by (a) the molecular structure of the surfactant and (b) the conditions under which the foam was generated. In the first case we varied the chain length and the head group size. In the second case we varied the surfactant concentration, the porosity of the disk through which the gas was supplied, and the gas flow rate Q.

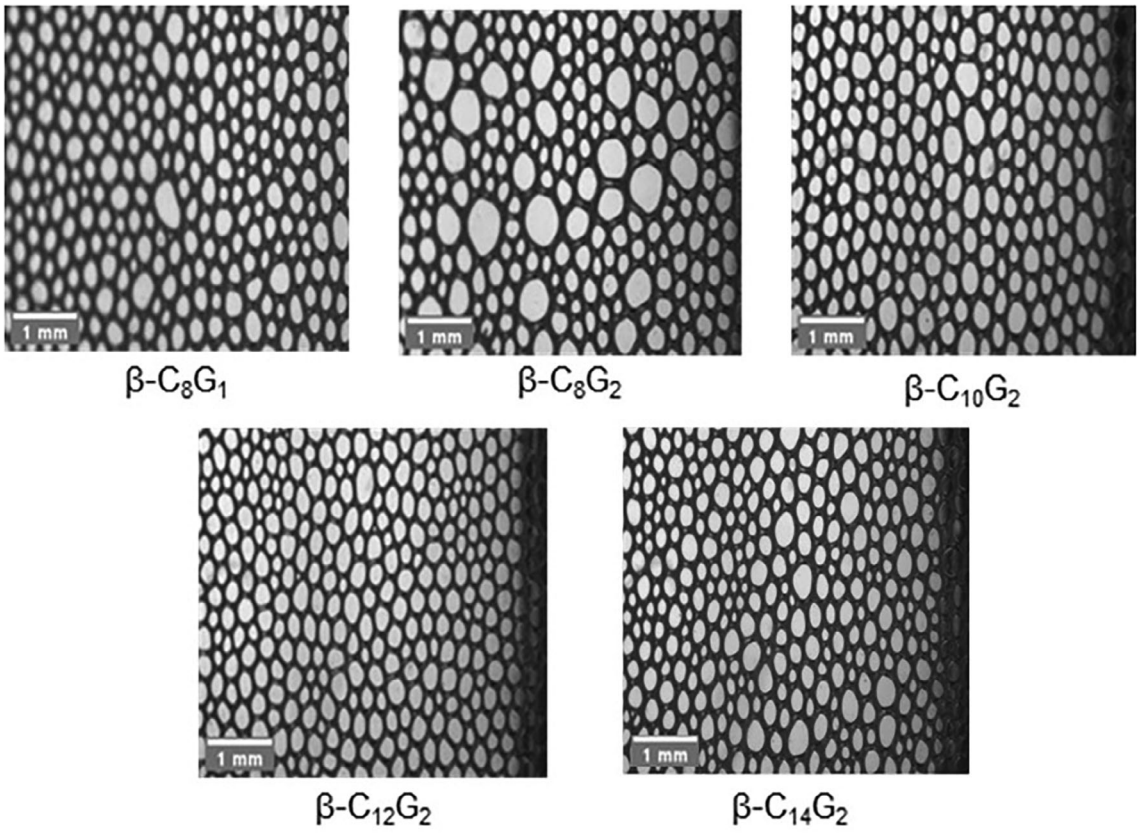

FIGURE 1 Pictures taken with the cell size analysis camera at $t = 0$ s for different surfactant solutions. All foams were generated with a porous disk with porosity P2. The concentrations of β-C_8G_1, β-C_8G_2, and β-$C_{14}G_2$ were 10 cmc, while for β-$C_{10}G_2$ and β-$C_{12}G_2$ 5 cmc were chosen.

Table 1 lists the surfactants that we used as well as the conditions under which the foams were generated. In addition, the values of the mean bubble radii <r > and of the polydispersity index *PI* are given, which were measured at different times from $t = 0$ s to $t = 1000$ s. A comparison of the polydispersity indices is shown in Figure S12.

The surfactants β-C_8G_1 and β-C_8G_2

We measured the foaming properties of aqueous surfactant solutions of β-C_8G_1 and β-C_8G_2. The measuring conditions were chosen as follows: the surfactant concentration was 10 cmc, a disk of porosity P2 was used, and the gas flow rate was $Q = 84$ mL min^{-1}. Figure 2a shows the foam volume V_{foam} as function of time *t*, while Figure 2b shows the time evolution of the liquid fraction *ε*.

Note that in Figure 2a the time $t = 0$ s corresponds to the time at which a foam volume of 120 mL is reached, and the gas flow stopped as explained in the Section 2. Assuming that the foam destabilization processes (drainage, coalescence, and coarsening) do not happen at $t < 0$, the growing part of the curve represents the foamability, while data measured for $t > 0$ can be assigned to the foam stability. This assumption was made for all experiments carried out in the study at hand.

Looking at Figure 2a one sees that the foamability of both surfactants is the same with a value of 86 s for 120 mL. Once the gas flow is switched off at $t = 0$, the foam of both samples collapses very rapidly. Comparing the two surfactants, one sees that the foam generated with β-C_8G_1 decays faster than the one generated with β-C_8G_2. Thus, for a given chain length, the additional sugar unit in the head group of β-C_8G_2 leads to a more stable foam.

TABLE 1 The table lists the used surfactants and the foam generation conditions.

	$t = 0$ s		$t = 0$ s		
Surfactant	**β-C_8G_1**	**β-C_8G_2**	**β-$C_{10}G_2$**	**β-$C_{12}G_2$**	**β-$C_{14}G_2$**
Concentration (c/cmc)	10	10	5	5	10
Disk Porosity	P2	P2	P2	P2	P2
Q (mL min^{-1})	84	84	60	60	60
<*r* > (mm)	0.22	0.25	0.22	0.17	0.20
PI	0.17	0.15	0.16	0.24	0.21
	$t = 50$ s		$t = 250$ s		
Surfactant	**β-C_8G_1**	**β-C_8G_2**	**β-$C_{10}G_2$**	**β-$C_{12}G_2$**	**β-$C_{14}G_2$**
Concentration (c/cmc)	10	10	5	5	10
Disk Porosity	P2	P2	P2	P2	P2
Q (mL min^{-1})	84	84	60	60	60
<*r* > (mm)	0.22	0.25	0.22	0.17	0.19
PI	0.21	0.16	0.16	0.27	0.23
	$t = 100$ s		$t = 500$ s		
Surfactant	**β-C_8G_1**	**β-C_8G_2**	**β-$C_{10}G_2$**	**β-$C_{12}G_2$**	**β-$C_{14}G_2$**
Concentration (c/cmc)	10	10	5	5	10
Disk porosity	P2	P2	P2	P2	P2
Q (mL min^{-1})	84	84	60	60	60
<*r* > (mm)	0.22	0.25	0.22	0.16	0.19
PI	0.24	0.17	0.17	0.31	0.23
	$t = 200$ s		$t = 1000$ s		
Surfactant	**β-C_8G_1**	**β-C_8G_2**	**β-$C_{10}G_2$**	**β-$C_{12}G_2$**	**β-$C_{14}G_2$**
Concentration (c/cmc)	10	10	5	5	10
Disk porosity	P2	P2	P2	P2	P2
Q (mL min^{-1})	84	84	60	60	60
<*r* > (mm)	0.23	0.25	0.22	0.16	0.19
PI	0.33	0.17	0.20	0.38	0.25

Note: Foams analyzed were generated at similar concentrations, porosities and gas flow rates *Q*. Mean bubble radii <*r*> and polydispersity indices *PI* are given for different times after foam generation.

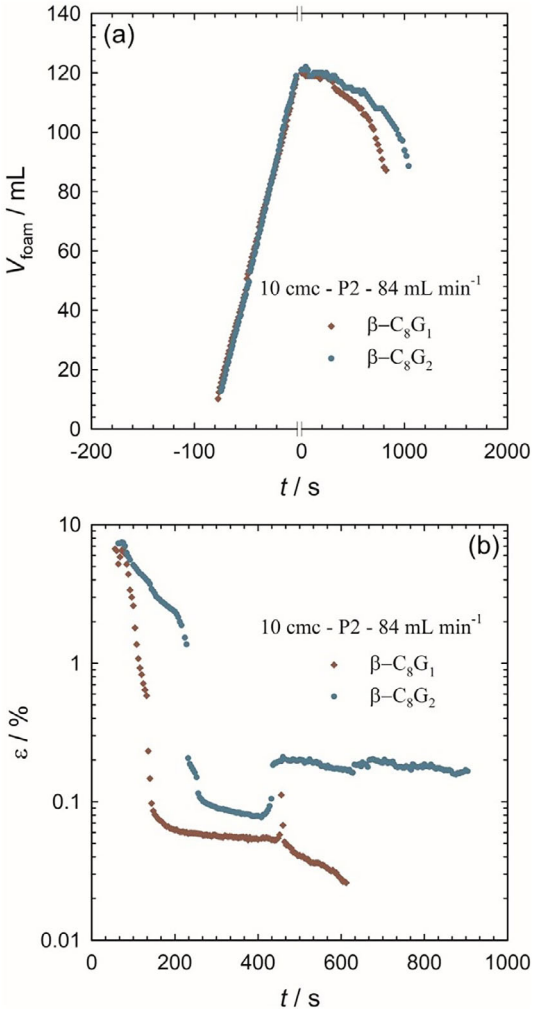

FIGURE 2 Variation of foam volume V_{foam} (a) and liquid fraction ε (b) of foams stabilized by β-C_8G_1 and β-C_8G_2 as function of time *t*. 60 mL of surfactant solution with a concentration of 10 cmc was sparged with N_2 at 84 mL min^{-1} to form a preset foam volume of 120 mL. The time $t = 0$ s represents the time at which V_{foam} reaches 120 mL. A disk with porosity P2 was used.

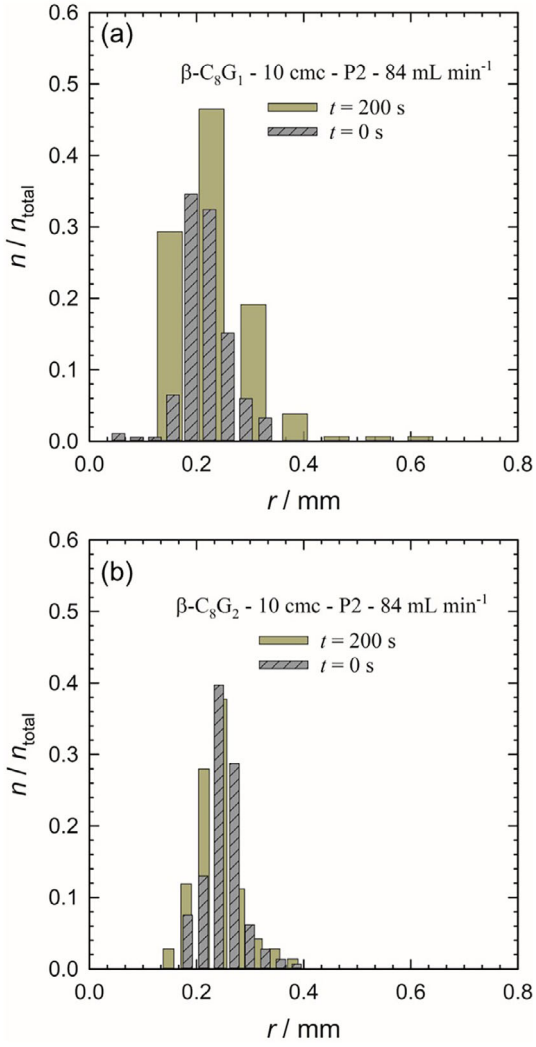

FIGURE 3 Relative number of bubbles n/n_{total} with different radii *r* for foams stabilized by β-C_8G_1 (a) and β-C_8G_2 (b), respectively. A surfactant concentration of 10 cmc, a gas flow rate of 84 mL min^{-1} and a disk with porosity P2 were used.

Looking at Figure 2b, one can see that the initial liquid fraction of both foams is approximately the same, namely ε ∼ 7%. The time evolution, however, is slightly different: the liquid fraction of the foam stabilized with β-C_8G_1 decreases faster, which, in turn, is in line with Figure 2a. Finally, the evolution of the bubble size distribution (see Figure 3) is also in line with a lower stability of the foam stabilized with β-C_8G_1. Looking at Figure 3 one clearly sees that the bubble size distribution shown in Figure 3a for β-C_8G_1 gets more polydisperse than the one shown in Figure 3b for β-C_8G_2, which is due to a faster aging of the foam.

In conclusion one can say that with both surfactant solutions one can only generate unstable foams that drain and thus decay quickly once the gas flow is switched off. The additional sugar unit in the head group, however, obviously increases the foam stability. This observation is perfectly in line with the fact that sugar surfactants form intersurfactant H-bonds between the head groups (Kanduč et al., 2021; Ranieri et al., 2018; Stubenrauch et al., 2017). A maltoside unit can form more H-bonds with its neighbor than a glucose unit. Thus, in the former case, the surfactant monolayer is more densely packed and more stable, which, in turn, leads to a more stable foam.

The surfactant β-$C_{10}G_2$

The foaming conditions listed in Table 1 were applied to solutions of β-$C_{10}G_2$. Measurements with the corresponding glucoside β-$C_{10}G_1$ were not

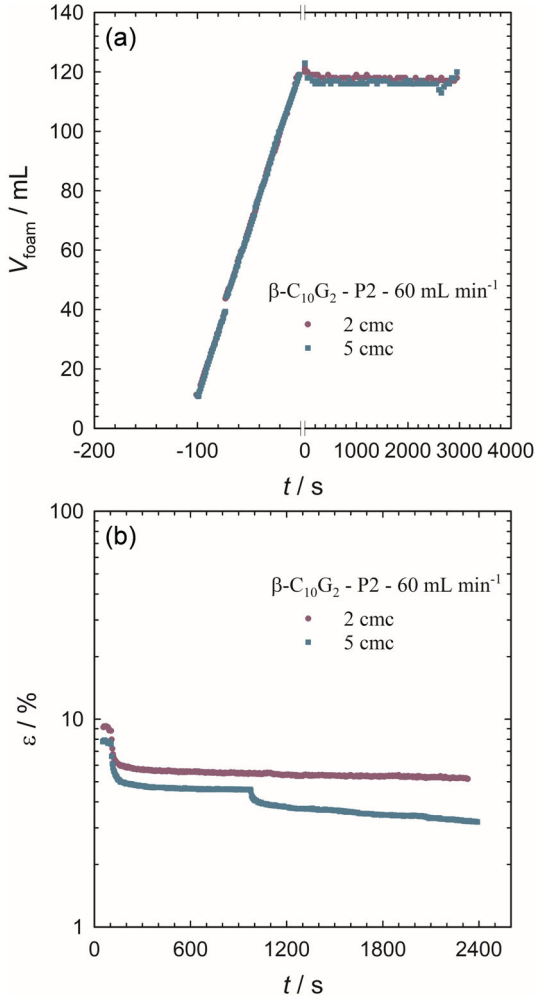

FIGURE 4 Variation of foam volume V_{foam} (a) and liquid fraction ε (b) of foams stabilized by β-$C_{10}G_2$ as function of time *t*. 60 mL of surfactant solution with a concentration of 2 and 5 cmc was sparged with N_2 at 60 mL min^{-1} to form a preset foam volume of 120 mL. The time $t = 0$ s represents the time at which V_{foam} reaches 120 mL. A disk with porosity P2 was used.

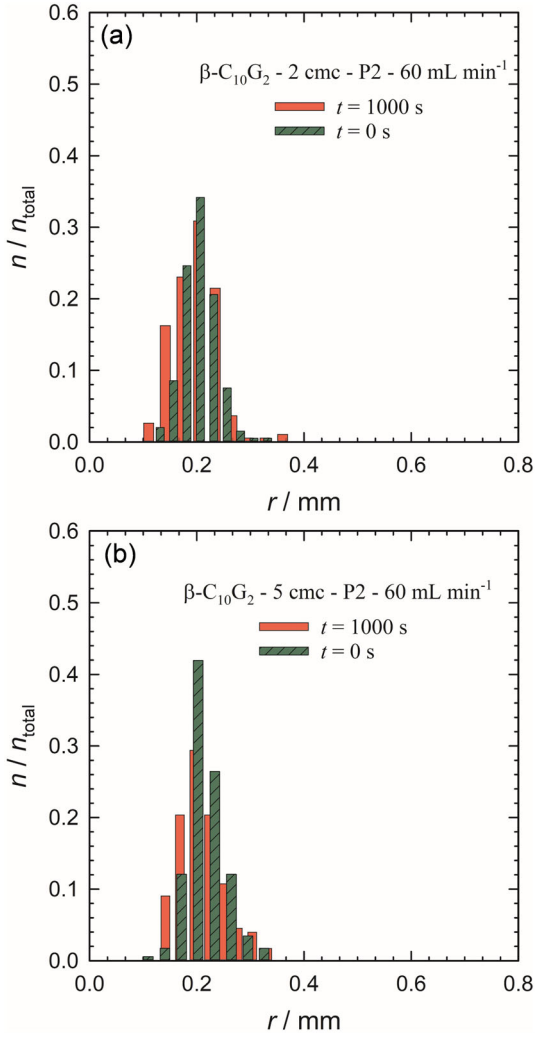

FIGURE 5 Relative number of bubbles n/n_{total} with different radii *r* for foams stabilized by β-$C_{10}G_2$ with a surfactant concentration of 2 cmc (a) and 5 cmc (b), respectively. A gas flow rate of 60 mL min^{-1} and a disk with porosity P2 were used.

possible due to the low solubility (Boyd et al., 2000), that is, the preparation of clear solutions with c > cmc were not possible (see Figure S2). In case of β-$C_{10}G_2$, the surfactant concentrations were 2 and 5 cmc, a disk of porosity P2 was used, and the gas flow rate was 60 mL min^{-1}. Figure 4a presents the foam volume V_{foam} as function of time *t*, while Figure 4b shows the time evolution of the liquid fraction *ε*.

At first one sees that the foamability of both surfactant solutions is basically the same, that is, 120 mL foam were generated in 120 s. Once switching off the gas, the foam volumes of both samples stayed constant during the experiment time of 3600 s.

Taking a look at Figure 4b, one can see that the initial liquid fraction of both foams is really the same with ε ∼ 8%–9%. Differently from what is seen for β-C_8G_1 and β-C_8G_2, however, the liquid fraction of both foams barely changes with time, which is in line with Figure 4a. Finally, there is also no time evolution of the bubble size distribution (see Figure 5), which means that neither drainage nor coalescence play a significant role during the first 1000s.

Comparing β-C_8G_2 and β-$C_{10}G_2$, one can see that foams stabilized with β-$C_{10}G_2$ are much more stable than those stabilized with β-C_8G_2. This difference in stability can be assigned to the fact that the surfactant layer can pack more densely for longer alkyl chain due to the increasing van der Waals interactions. The increase of the packing density and the lowering of the surface roughness lead to an increase of the surface elasticity (Bergeron, 1999; Stubenrauch et al., 2017) and thus of the foam stability (Georgieva et al., 2009; Stubenrauch et al., 2010).

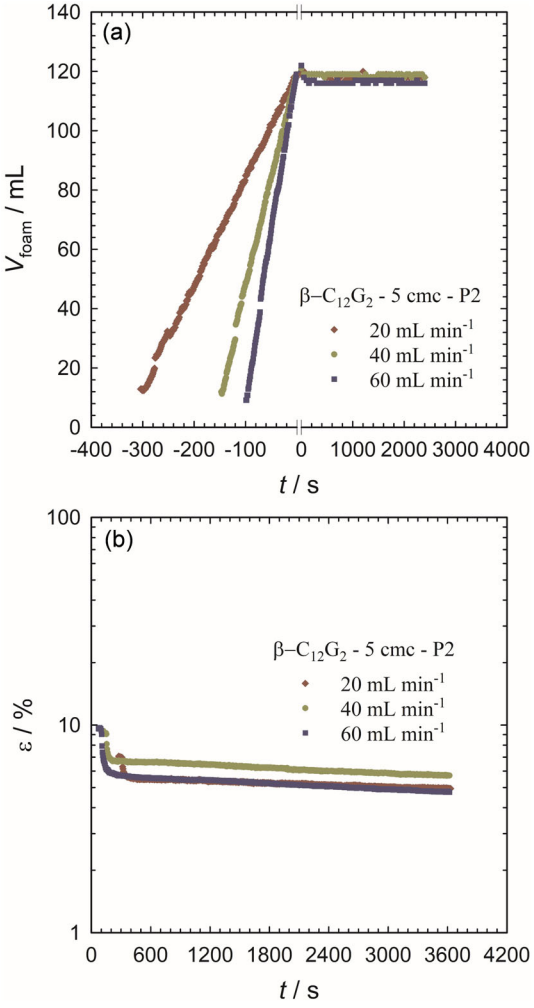

FIGURE 6 Variation of foam volume V_{foam} (a) and liquid fraction ε (b) of foams stabilized by β-$C_{12}G_2$ as function of time t. 60 mL of surfactant solution with a concentration of 5 cmc was sparged with N_2 at 20, 40, and 60 mL min^{-1} to form a preset foam volume of 120 mL. The time $t = 0$ s represents the time at which V_{foam} reaches 120 mL. A disk with porosity P2 was used.

The surfactant β-$C_{12}G_2$

The conditions for foam generation with aqueous solutions of β-$C_{12}G_2$ were as follows: the surfactant concentrations were 2 and 5 cmc, disks of porosities P1, P2, and P3 were used, and the gas flow rates chosen were 20, 40, and 60 mL min^{-1}. Measurements with the corresponding glucoside β-$C_{12}G_1$ were not possible due to the low solubility (Boyd et al., 2000), that is, the preparation of clear solutions with c > cmc were not possible (see Figure S3). In Figure 6a one sees the foam volume V_{foam} as function of time t for foams generated with three different flow rates. The surfactant concentration was c = 5 cmc and the disk porosity was P2. Figure 6b shows the time evolution of the liquid fraction ε at the same conditions. Additional data for 2 cmc and different disk porosities are shown in Figures S4–S8.

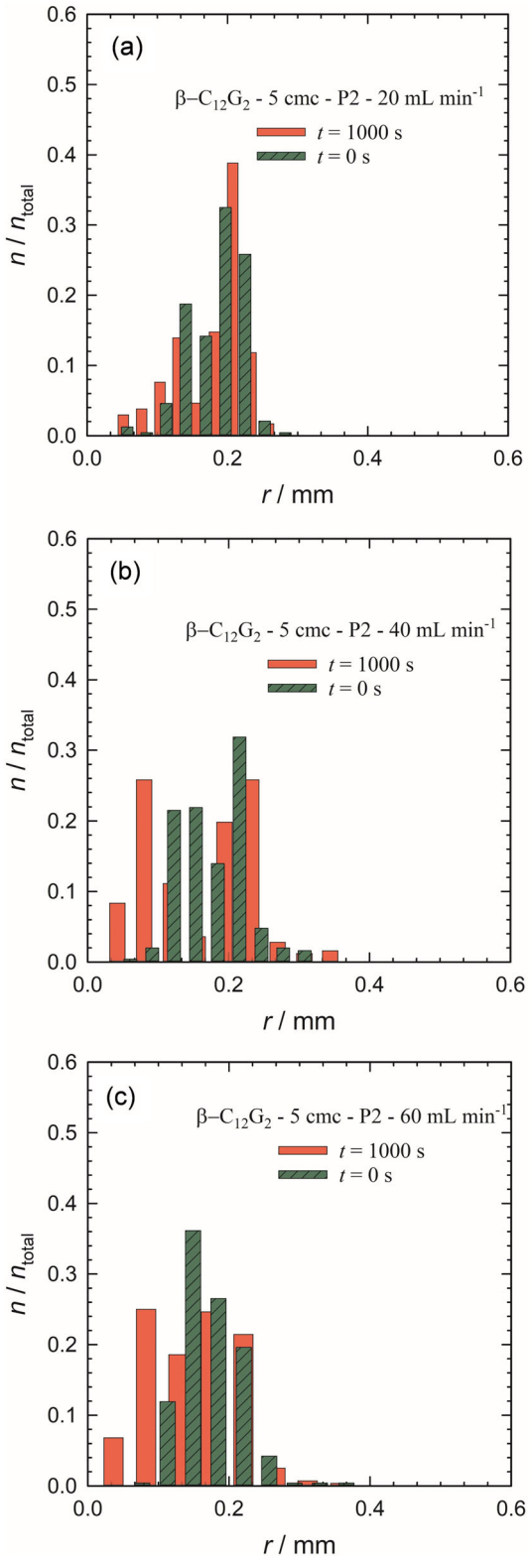

FIGURE 7 Relative number of bubbles n/n_{total} with different radii r for foams stabilized by β-$C_{12}G_2$ with a surfactant concentration of 5 cmc. Gas flow rates of (a) 20 mL min^{-1} (b) 40 mL min^{-1}, and (c) 60 mL min^{-1} and a disk with porosity P2 were used.

First, evaluating foamability, one notices that the foam volume increases linearly with values of 6, 3 and 2 min for 120 mL of foam for 20, 40, and 60 mL min^{-1}

respectively. As expected, the lower the flow rate the longer it takes to generate 120 mL of foam. As regards foam stability, like it was the case for β-$C_{10}G_2$, the foam volume remains constant at 120 mL during the whole experiment. Thus, the flow rate has an influence on the foamability only and not on the foam stability.

Looking at Figure 6b, one can see different initial liquid fractions attributed for different gas flow rates, namely $\varepsilon \sim 7.0$, 9.0 and 9.7% for 20, 40, and 60 mL min^{-1} respectively. This trend is more pronounced at surfactant concentration of 2 cmc (Figure S4e): $\varepsilon \sim 3.7$, 6.4 and 8.0% for 20, 40, and 60 mL min^{-1} respectively. This observation is also expected: the lower the flow rate, the longer it takes to generate 120 mL of foam. Since drainage cannot be avoided during foam generation, the foam generated with the lowest flow rate has the longer time for drainage, which, in turn results in the lowest initial liquid fraction. In all cases one observed a fast drainage in the first couple of minutes which than levels off as was the case for β-$C_{10}G_2$. Finally, the evolution of the bubble size distribution (see Figure 7) is in line with the high foam stability: bubble size distribution does not change significantly during the first 1000 s, that is, aging effects such as coarsening and coalescence do not play a significant role.

The presented data are in agreement with previous studies (Boos et al., 2012; Stubenrauch et al., 2009) in which the very same surfactant was studied. In both studies the foam volume did not change during the experiment, while all foams drained significantly.

The study at hand differs from the previous one because here we studied systematically the influence of the foaming conditions (different flow rates and different porosities) for two different concentrations (2 cmc and 5 cmc). Under all conditions very stable foams were generated. In other words, foams stabilized by β-$C_{12}G_2$ no matter what the foaming conditions are. It was only for 2 cmc where we observed a small influence of the disk porosity (see Figure S4c,f as well as Figure S7d–f). Foams generated at 2 cmc with a disk of porosity P3 were less stable and the bubble size distribution became more polydisperse after 1000 s compared to all other foams. There are two reasons for this difference. (1) Depletion: The bubbles generated with a P3 disk are the smallest, that is, here the largest water-air interface is generated. For this large interface the surfactant concentration is too low to fully cover the new surface without changing the bulk concentration (Boos et al., 2012). We estimated this concentration changing Δc with eq. (7) from Boos et al. (2012) for our experiment conditions.

$$\frac{\Delta c}{\mathrm{cmc}} = \frac{1}{\mathrm{cmc}} \frac{3}{A_{\mathrm{mol}} N_A} \frac{1}{r_{32}} \frac{V_{\mathrm{foam}}}{V_{\mathrm{solution}}}, \quad (4)$$

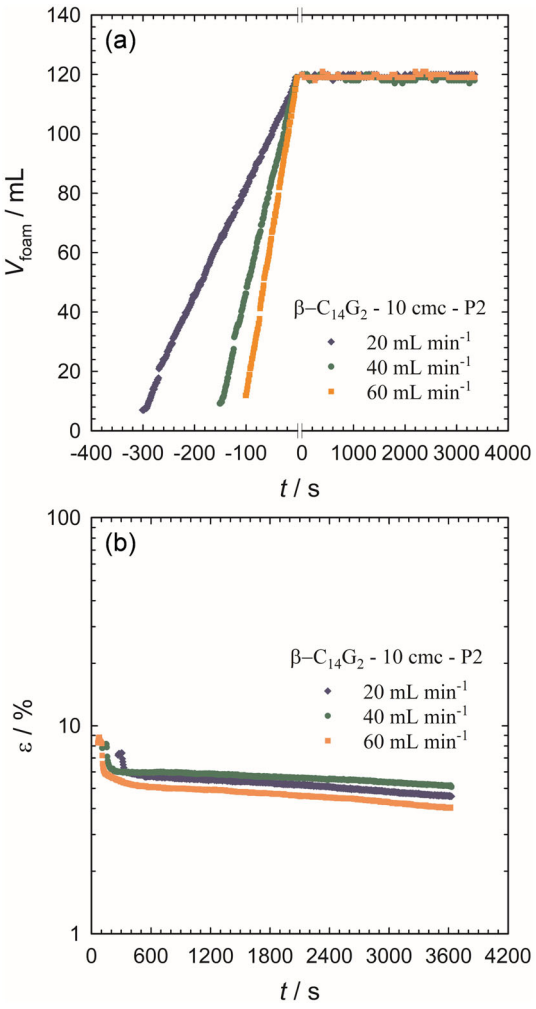

FIGURE 8 Variation of foam volume V_{foam} (a) and liquid fraction ε (b) of foams stabilized by β-$C_{14}G_2$ as function of time *t*. 60 mL of surfactant solution with a concentration of 10 cmc was sparged with N_2 at 20, 40, and 60 mL min^{-1} to form a preset foam volume of 120 mL. The time $t = 0$ s represents the time at which V_{foam} reaches 120 mL. A disk with porosity P2 was used.

with the area per surfactant molecule A_{mol}, Avogadro's number N_A, the Sauter mean radius $r_{32} = <r^3>/<r^2>$, and the volume of foam V_{foam} and surfactant solution $V_{solution}$, respectively. After foam generation the bulk concentration of β-$C_{12}G_2$ is ∼ cmc, that is, half of the surfactant is absorbed at the newly generated surface. (2) Coarsening: The smaller the bubbles, the larger is the Laplace pressure and thus the faster is coarsening.

The surfactant β-$C_{14}G_2$

The conditions for foam generation with aqueous solutions of β-$C_{14}G_2$ were as follows: the surfactant concentration was 10 cmc, disks of porosities P1, P2, and P3

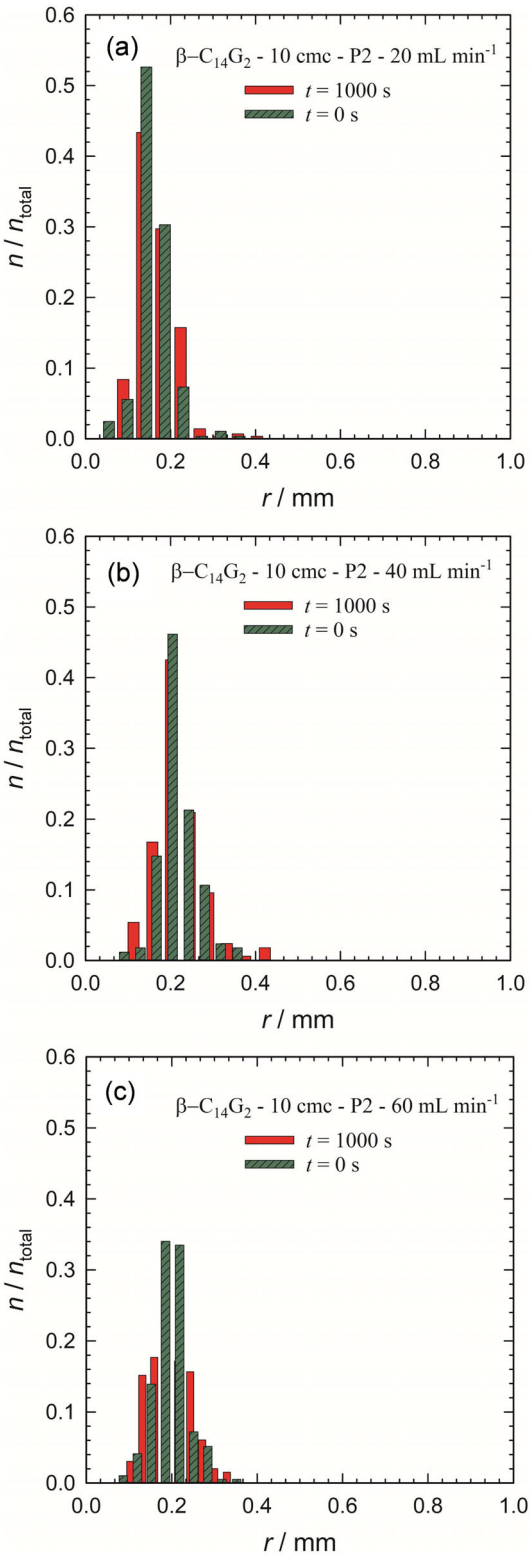

FIGURE 9 Relative number of bubbles n/n_{total} with different radii r for foams stabilized by β-$C_{14}G_2$ with a surfactant concentration of 10 cmc. Gas flow rates of (a) 20 mL min^{-1} (b) 40 mL min^{-1}, and (c) 60 mL min^{-1} and a disk with porosity P2 were used.

were used, and the gas flow rates chosen were 20, 40, and 60 mL min^{-1}. Considering that β-$C_{14}G_2$ is part of the same surfactant family, one expects similar qualitative results as for β-$C_{10}G_2$ and β-$C_{12}G_2$. In Figure 8a one sees the foam volume V_{foam} as function of time t at the different flow rates and disk of porosity P2, while Figure 8b shows the time evolution of the liquid fraction ε at the same conditions. All other data are shown in the Supporting Information in Figures S9–S11.

As regards the foamability we measured the same values as for β-$C_{12}G_2$, namely 6, 3, and 2 min for the generation of 120 mL foam with flow rates of 20, 40, and 60 mL min^{-1}, respectively. Again, the foams are very stable which is reflected in the constant foam volume (Figure 8a) and in the constant bubble size distribution (Figure 9). The liquid fraction changes in the same way as was observed for β-$C_{12}G_2$: the initial liquid fraction is the lowest for the smallest flow rate, it changes rapidly during the first minutes and then levels off. A change of the foaming conditions (flow rates and disk porosities) has no influence on the foam stability (Figures S9–S11). Thus, again, foams stabilized by β-$C_{14}G_2$ are expected to be very stable no matter what the foaming conditions are. Note, that all measurements were carried out at 10 cmc. Because of the very low cmc of the for β-$C_{14}G_2$ severe depletion effects are expected at lower surfactant concentrations.

CONCLUSIONS

If one wants to use a surfactant for a broad variety of foam applications one must understand how it behaves under different foam generation conditions. This is exactly what this study is about: we generate foam with a family of sugar-based surfactants under a broad variety of conditions. The structure of the five alkyl polyglucosides varied either in the length of the alkyl chain or in the number of glucose groups. The experimental conditions varied as regards the bulk concentrations (2, 5, and 10 cmc), the disk porosities (P1, P2, and P3), and the N_2 flow rates (20, 40, 60, and 84 mL min^{-1}). The study was conducted with the foam analyzer FoamScan, with which foamability and foam stability can be measured by monitoring how the foam volume, the liquid content, and the bubble size distribution change with time.

We observed a good foamability of all surfactant solutions without any significant destabilizing effects during foam generation. As regards foam stability, we found that foams generated with β-C_8G_1 decay faster than those generated with β-C_8G_2. Since the two surfactants have the same chain length, it is the extra sugar unit in the head group of β-C_8G_2 that leads to a more stable foam. This observation can be explained by the formation of more H-bonds between neighboring head groups.

For β-$C_{10}G_2$, β-$C_{12}G_2$, and β-$C_{14}G_2$, the foamability and foam stability were basically the same. Other than for β-C_8G_1 and β-C_8G_2, the foam volume does not change over 3600 s, i.e. that neither coalescence nor coarsening

played a significant role during the experiment. The addition of one glucose group in the head group and the enlargement of the alkyl chain increases significantly the foam stability. First, strong intersurfactant H-bonds between neighboring head groups are formed at the surface, which, in turn, increases the packing density and thus the foam stability. Second, the longer the chain length the stronger are the attractive van der Waals forces which, again, increases the packing density and the foam stability.

From an industrial point of view, our study helps to understand properties of foams generated under different conditions. For the special surfactant family investigated here, a very good performance can be expected for various foam generation conditions as long as the hydrophobic chain has 10 or more C-atoms. We conclude with a qualitative order for foam stability: β-C_8G_1 < β-C_8G_2 << β-$C_{10}G_2$ < ~ β-$C_{12}G_{12}$ < ~ β-$C_{14}G_2$.

AUTHOR CONTRIBUTIONS

João Victor Cordeiro do Nascimento: Investigation; measurements; data analysis; original draft. **Natalie Preisig**: Data analysis; writing; editing. **Eduardo R. A. Lima:** Supervision; review; editing. **Cosima Stubenrauch**: Conceptualization; supervision; review; editing, writing. All authors contributed to and approved the final draft of the manuscript.

ACKNOWLEDGMENTS

This study was financed in part by the Coordenação de Aperfeiçoamento de Pessoal de Nível Superior-Brasil (CAPES)-Finance Code 001.

CONFLICT OF INTEREST STATEMENT

The authors declare that they have no conflict of interest.

DATA AVAILABILITY STATEMENT

The data that support the findings of this study are available from the corresponding author upon reasonable request.

ETHICS STATEMENT

No human or animals were used in this research.

ORCID

Cosima Stubenrauch https://orcid.org/0000-0002-1247-4006

REFERENCES

Andrieux S, Quell A, Stubenrauch C, Drenckhan W. Liquid foam templating: a route to tailor-made polymer foams. Adv Colloid Interface Sci. 2018;256:276–90. https://doi.org/10.1016/j.cis.2018.03.010

Bergeron V. Forces and structure in thin liquid soap films. J Phys Condens Matter. 1999;11(19):R215–38. https://doi.org/10.1088/0953-8984/11/19/201

Bhadani A, Kafle A, Ogura T, Akamatsu M, Sakai K, Sakai H, et al. Current perspective of sustainable surfactants based on renewable building blocks. Curr Opin Colloid Interface Sci. 2020;45:124–35. https://doi.org/10.1016/j.cocis.2020.01.002

Bois R, Pezron I, Nesterenko A. Dynamic interfacial properties of sugar-based surfactants: experimental study and modeling. Colloids Interface Sci Commun. 2020;37:100293. https://doi.org/10.1016/j.colcom.2020.100293

Bois R, Pezron I, Rotureau P, Van Hecke E, Fayet G, Nesterenko A. Foaming behavior of sugar-based surfactants: influence of molecular structure and anticipation from surface properties. J Dispers Sci Technol. 2023;44(5):840–51. https://doi.org/10.1080/01932691.2021.1974877

Boos J, Drenckhan W, Stubenrauch C. On how surfactant depletion during foam generation influences foam properties. Langmuir. 2012;28(25):9303–10. https://doi.org/10.1021/la301140z

Boos J, Drenckhan W, Stubenrauch C. Protokol for studying aqueous foams stabilized by surfactant mixtures. J Surfact Deterg. 2013;16(1):1–12. https://doi.org/10.1007/s11743-012-1416-2

Boos J, Preisig N, Stubenrauch C. Dilational surface rheology studies of n-dodecyl-β-d-maltoside, hexaoxyethylene dodecyl ether, and their 1:1 mixture. Adv Colloid Interface Sci. 2013;197–198:108–17. https://doi.org/10.1016/j.cis.2013.05.001

Boyd BJ, Drummond CJ, Krodkiewska I, Grieser F. How chain length, headgroup polymerization, and anomeric configuration govern the thermotropic and lyotropic liquid crystalline phase behavior and the air−water interfacial adsorption of glucose-based surfactants. Langmuir. 2000;16(19):7359–67. https://doi.org/10.1021/la991573w

Carnero Ruiz C. Sugar-based surfactants: fundamentals and applications. Boca Raton, FL:CRC Press; 2008. https://doi.org/10.1201/9781420051674

Ekserova DR, Kruglīākov PM. Foam and foam films: theory, experiment, application. Amsterdam, Netherlands: Elsevier; 1998.

Encyclopedia of chemical technology. 12: Fo—Gr. 5th ed. Hoboken, NJ: Wiley; 2005.

Engels T, Rybinski W, Schmiedel P. Structure and dynamics of surfactant-based foams. In: Rehage EH, Peschel G, editors. Structure, dynamics and properties of disperse colloidal systems. Volume 111. Germany: Springer-Verlag Berlin Heidelberg GmbH; 1998. p. 117–26. https://doi.org/10.1007/BFb0118120

Feitosa K, Marze S, Saint-Jalmes A, Durian DJ. Electrical conductivity of dispersions: from dry foams to dilute suspensions. J Phys Condens Matter. 2005;17:6301–5. https://doi.org/10.1088/0953-8984/17/41/001

Gaudin T, Fayet G, Rotureau P, Pezron I. Anticipating dissolution issues of sugar-based surfactants through a decision tree approach. J Surfactant Deterg. 2018;21(6):835–43. https://doi.org/10.1002/jsde.12178

Gaudin T, Lu H, Fayet G, Berthauld-Drelich A, Rotureau P, Pourceau G, et al. Impact of the chemical structure on amphiphilic properties of sugar-based surfactants: a literature overview. Adv Colloid Interface Sci. 2019;270:87–100. https://doi.org/10.1016/j.cis.2019.06.003

Gaudin T, Rotureau P, Pezron I, Fayet G. New QSPR models to predict the critical micelle concentration of sugar-based surfactants. Ind Eng Chem Res. 2016;55(45):11716–26. https://doi.org/10.1021/acs.iecr.6b02890

Gaudin T, Rotureau P, Pezron I, Fayet G. Investigating the impact of sugar-based surfactants structure on surface tension at critical micelle concentration with structure-property relationships. J Colloid Interface Sci. 2018;516:162–71. https://doi.org/10.1016/j.jcis.2018.01.051

Gaudin T, Rotureau P, Pezron I, Fayet G. Estimating the adsorption efficiency of sugar-based surfactants from QSPR models. Int J

Quant Struct Prop Relationships. 2019;4(2):28–51. https://doi.org/10.4018/IJQSPR.2019040102
Georgieva D, Cagna A, Langevin D. Link between surface elasticity and foam stability. Soft Matter. 2009;5(10):2063. https://doi.org/10.1039/b822568k
Grigoriev D, Stubenrauch C. Surface elasticities of aqueous β-dodecyl-d-maltoside solutions: a capillary wave study. Colloids Surf A Physicochem Eng Asp. 2007;296(1–3):67–75. https://doi.org/10.1016/j.colsurfa.2006.09.025
Hill K, Rhode O. Sugar-based surfactants for consumer products and technical applications. Lipid Fett. 1999;101(1):25–33. https://doi.org/10.1002/(SICI)1521-4133(19991)101:1<25::AID-LIPI25>3.0.CO;2-N
Kanduč M, Schneck E, Stubenrauch C. Intersurfactant H-bonds between head groups of n-dodecyl-β-d-maltoside at the air-water interface. J Colloid Interface Sci. 2021;586:588–95. https://doi.org/10.1016/j.jcis.2020.10.125
Kim Y-H, Koczo K, Wasan DT. Dynamic film and interfacial tensions in emulsion and foam systems. J Colloid Interface Sci. 1997;187(1):29–44. https://doi.org/10.1006/jcis.1996.4507
Lourith N, Kanlayavattanakul M. Natural surfactants used in cosmetics: glycolipids. Int J Cosmet Sci. 2009;31(4):255–61. https://doi.org/10.1111/j.1468-2494.2009.00493.x
Muruganathan R, Krustev R, Müller H-J, Möhwald H, Kolaric B, Klitzing RV. Foam films stabilized by dodecyl maltoside. 1. Film thickness and free energy of film formation. Langmuir. 2004;20(15):6352–8. https://doi.org/10.1021/la0494268
Prins A. Surface rheology and practical behaviour of foams and thin liquid films. Chem Ing Tech. 1992;64(1):73–5. https://doi.org/10.1002/cite.330640116
Prud'homme RK, Khan SA. Foams: theory, measurements, and applications. New York: Marcel Dekker, Inc; 1996.
Pugh RJ. Foaming, foam films, antifoaming and defoaming. Adv Colloid Interface Sci. 1996;64:67–142. https://doi.org/10.1016/0001-8686(95)00280-4
Ranieri D, Preisig N, Stubenrauch C. On the influence of intersurfactant H-bonds on foam stability: a study with technical grade surfactants. Tenside Surfact Det. 2018;55(1):6–16. https://doi.org/10.3139/113.110537
Rojas OJ, Stubenrauch C, Lucia LA, Habibi Y. Interfacial properties of sugar-based surfactants. Bio-based surfactants and detergents: synthesis, properties and applications. Volume 457. Urbana: AOCS Press; 2009.
Rosen MJ. Surfactants and interfacial phenomena. 3rd ed. Hoboken, NJ: Wiley-Interscience; 2004.
Rossen WR. Foams in enhanced oil recovery. Em Foams: Amsterdam, Netherlands: Routledge; 1996.
Sadoc JF, Rivier N. Foams and emulsions. Springer Netherlands; 1999. https://doi.org/10.1007/978-94-015-9157-7
Saint-Jalmes A. Physical chemistry in foam drainage and coarsening. Soft Matter. 2006;2(10):836–49. https://doi.org/10.1039/b606780h
Santini E, Ravera F, Ferrari M, Stubenrauch C, Makievski A, Krägel J. A surface rheological study of non-ionic surfactants at the water–air interface and the stability of the corresponding thin foam films. Colloids Surf A Physicochem Eng Asp. 2007;298(1–2):12–21. https://doi.org/10.1016/j.colsurfa.2006.12.004
Shinoda K, Yamaguchi T, Hori R. The surface tension and the critical micelle concentration in aqueous solution of β-D-alkyl glucosides and their mixtures. Bull Chem Soc Jpn. 1961;34(2):237–41. https://doi.org/10.1246/bcsj.34.237
Stubenrauch C. Sugar surfactants—aggregation, interfacial, and adsorption phenomena. Curr Opin Colloid Interface Sci. 2001;6(2):160–70. https://doi.org/10.1016/S1359-0294(01)00080-2
Stubenrauch C, Claesson PM, Rutland M, Manev E, Johansson I, Pedersen JS, et al. Mixtures of n-dodecyl-β-d-maltoside and hexaoxyethylene dodecyl ether—surface properties, bulk properties, foam films, and foams. Adv Colloid Interface Sci. 2010;155(1–2):5–18. https://doi.org/10.1016/j.cis.2009.12.002
Stubenrauch C, Cohen R, Exerowa D. A pH-study of *n*-dodecyl-β-D-maltoside foam films. Langmuir. 2007;23(4):1684–93. https://doi.org/10.1021/la062310m
Stubenrauch C, Hamann M, Preisig N, Chauhan V, Bordes R. On how hydrogen bonds affect foam stability. Adv Colloid Interface Sci. 2017;247:435–43. https://doi.org/10.1016/j.cis.2017.02.002
Stubenrauch C, Menner A, Bismarck A, Drenckhan W. Emulsion and foam templating—promising routes to tailor-made porous polymers. Angew Chem Int Ed. 2018;57(32):10024–32. https://doi.org/10.1002/anie.201801466
Stubenrauch C, Miller R. Stability of foam films and surface rheology: an oscillating bubble study at low frequencies. J Phys Chem B. 2004;108(20):6412–21. https://doi.org/10.1021/jp049694e
Stubenrauch C, Shrestha LK, Varade D, Johansson I, Olanya G, Aramaki K, et al. Aqueous foams stabilized by n-dodecyl-β-d-maltoside, hexaethyleneglycol monododecyl ether, and their 1: 1 mixture. Soft Matter. 2009;5(16):3070. https://doi.org/10.1039/b903125a
Tadros TF. Colloid stability: the role of surface forces. Hoboken, NJ: Wiley-VCH Verlag; 2007.
Tamura T, Kaneko Y, Ohyama M. Dynamic surface tension and foaming properties of aqueous polyoxyethylene n-dodecyl ether solutions. J Colloid Interface Sci. 1995;173(2):493–9. https://doi.org/10.1006/jcis.1995.1351
Tesmann H, Kahre J, Hensen H, Salka BA. Alkyl polyglycosides in personal care products. In: Hill EK, von Rybinski W, Stoll G, editors. Alkyl polyglycosides. 1st ed. Hoboken, NJ: Wiley; 1996. p. 71–98. https://doi.org/10.1002/9783527614691.ch5
Ting L, Wasan DT, Miyano K, Xu S-Q. Longitudinal surface waves for the study of dynamic properties of surfactant systems. II. Air-solution interface. J Colloid Interface Sci. 1984;102(1):248–59. https://doi.org/10.1016/0021-9797(84)90217-0
Von Rybinski W, Hill K. Alkyl Polyglycosides—properties and applications of a new class of surfactants. Angew Chem Int Ed. 1998;37(10):1328–45. https://doi.org/10.1002/(SICI)1521-3773(19980605)37:10<1328::AID-ANIE1328>3.0.CO;2-9
Ware AM, Waghmare JT, Momin SA. Alkylpolyglycoside: carbohydrate based surfactant. J Dispers Sci Technol. 2007;28(3):437–44. https://doi.org/10.1080/01932690601107807
Weaire DL, Hutzler S. The physics of foams. Oxford, UK: Clarendon Press; 1999.
Yoshimura T, Umezawa S, Fujino A, Torigoe K, Sakai K, Sakai H, et al. Equilibrium surface tension, dynamic surface tension, and micellization properties of lactobionamide-type sugar-based Gemini surfactants. J Oleo Sci. 2013;62(6):353–62. https://doi.org/10.5650/jos.62.353
Zhao H, Sun H, Qi N, Li Y. Understanding of the foam capability of sugar-based nonionic surfactant from molecular level. Colloids Surf A Physicochem Eng Asp. 2018;551:165–73. https://doi.org/10.1016/j.colsurfa.2018.05.010

SUPPORTING INFORMATION

Additional supporting information can be found online in the Supporting Information section at the end of this article.

How to cite this article: do Nascimento JVC, Lima ERA, Preisig N, Stubenrauch C. Properties of liquid foams stabilized by sugar-based surfactants and prepared under different conditions. J Surfact Deterg. 2025;28(2):321–31. https://doi.org/10.1002/jsde.12800